A theoretical model of phospholipid dynamics in membranes

Alberta Ferrarini and Pier Luigi Nordio
Department of Physical Chemistry, University of Padua, 35131 Padova, Italy
Giorgio J. Moro
Institute of Physical Chemistry, University of Parma, 43100 Parma, Italy
Richard H. Crepeau and Jack H. Freed
Baker Laboratory of Chemistry, Cornell University, Ithaca, New York 14853

(Received 3 April 1989; accepted 27 July 1989)

Static and dynamic properties related to the internal configurational motions have been calculated for the alkyl chains of phospholipid molecules in a membrane environment in the liquid crystal phase. The calculations have been performed for the chain 1 of 1,2-dipalmitoyl 3-*sn*-phosphatidylcholine (DPPC), a typical constituent of phospholipid membranes. Under the assumption of fixed bond lengths and bond angles, the internal dynamics of the chain is described in terms of 15 dihedral angles. The time evolution of the angular variables is assumed to be diffusional in character, and a master equation for transitions among the stable conformers is constructed from the energetics and hydrodynamics of the chain. This method is an extension to the time domain of the rotational isomeric state (RIS) approximation, which has been widely used to compute static properties of the chains. After calculation of the suitable correlation functions, effective rate constants relevant for spectroscopic and kinetic observables have been computed, and the results have been compared with those obtained by recent Brownian dynamics (BD) calculations. The position dependence of the rate constants along the chain has been examined with special reference to understanding the effects resulting from cooperativity in the conformational transitions. The overall spinning and tumbling of the chain has also been described by a diffusive model. The calculated spectral densities for the composite motional process have been used to rationalize the behavior of the relaxation times T_1, T_2, and $T_{1\rho}$ measured in deuterium nuclear magnetic resonance (NMR) experiments.

I. INTRODUCTION

The calculation of the dynamical properties in molecular systems with many degrees of freedom is a formidable task even when the most advanced computer facilities are available. In the order of decreasing complexity, three methods can be employed: molecular dynamics (MD), Brownian dynamics (BD), and the master equation (ME) for conformational transitions.

MD requires the full calculation of trajectories for a statistically significant number of molecules, and it cannot be pushed to time scales longer than nanoseconds even for alkyl chains of hexane size.[1,2] In this way, the range of characteristic times for most configurational transitions is practically beyond the capability of the method.

BD remains a good alternative for molecular systems of the complexity of phospholipid chains, where it has been recently applied with good success. Pastor, Venable, and Karplus[3a] have, in fact, performed a BD calculation on chain 1 of DPPC, the other chains being assumed to participate in the effective interactions exerted by the surrounding medium. An extended atom model was assumed for the chain, with only the skeleton carbons, and not the hydrogen atoms, being explicitly considered. A systematic attempt was performed to fit the field parameters, related to the internal energy and the mean field interaction with the lipid environment, by comparing calculated and experimental order parameters. The actual number of computational steps in the simulations allows one to follow motions on the nanosecond time scale, at the cost of computational times of the order of a week. Besides the heavy requirements of computational time, BD shares with MD the problem of degradation of the numerical results when the technique is used to interpret processes occurring at long time scales.

In a second paper, Pastor, Venable, Karplus, and Szabo[3b] used these results to calculate NMR T_1 relaxation times. To do so, fast axial rotation and slow diffusive wobbling in a cone of the chain axis were superimposed on the internal motions. The motions were considered uncoupled, and the correlation functions for internal motions, obtained from the trajectory points, were fitted with a sum of a few exponentials.

The ME method is an extension to the time domain of the rotational isomeric state (RIS) approximation.[4] In the last 20 years, this approach was taken by numerous authors at different levels of sophistication. Wallach[5] assumed the multiple internal rotations to be completely factorized. Levine *et al.*[6] considered the anisotropy of the diffusion but adopted a single phenomenological rate constant for the internal motions. London and Avitabile[7] explicitly considered the energetics of the *trans-gauche* isomerism, while Wittebort and Szabo[8] abandoned the assumption of decoupled rotations but still used phenomenological transition rates. Edholm and Blomberg[9] first realized the necessity of applying Kramers theory for calculating the rates of chemical reactions to the specific case of conformational processes.

 0021-9606/89/215707-15$02.10

Helfand and Skolnick,[10] on the basis of a mathematical treatment proposed by Langer[11] for the solution of the multidimensional diffusion equation, emphasized the role of cooperativity effects in minimizing the frictional drag during the saddle point crossing, thereby avoiding the need to consider crankshaft or kink motions that, although energetically unfavored, appeared likely to occur for hydrodynamical reasons.[12,13] Ferrarini, Moro, and Nordio[14,15] used the concept of localized functions to project a multivariate diffusion equation in continuous torsional variables into a master equation for transitions among discrete sites, thereby giving the prescriptions for the evaluation of energetic and frictional terms without resorting to phenomenological parameters. The time evolution of the specific properties was expressed in the language of correlation functions, which leads quite naturally to the definition of effective kinetic constants.

In this work, we shall adopt the ME procedure to describe the conformational processes occurring in the aliphatic chains of phospholipid molecules and to interpret the NMR relaxation data available for these systems.

To appreciate the reasons which motivate our choice, a deeper comparison of the BD and ME methods is now in order. BD is a description of the dynamical processes suffered by a single probe molecule in a thermal bath. The method consists in the sampling of trajectories for the collection of particles constituting the molecular probe, subjected to a specified force field and to a rapidly fluctuating force that takes into account the interactions with the bath. The stochastic force is generally chosen in such a way as to reproduce diffusional regimes, i.e., conditions in which inertial effects are quenched by rapid thermalization of the momenta coordinates.

The BD method is an effective technique which averages many trajectories of the Langevin equation to obtain correlation functions instead of solving the multidimensional diffusion equation for the same system of particles. Numerical results identical to those offered by the BD method could, in principle, be obtained by a basis function expansion of the corresponding diffusion operator. In practice, however, eigenfunction expansions can be applied to diffusion equations with only a few coupled variables, because of the memory requirements for storing the matrix. Modern efficient algorithms which take full advantage of the matrix sparsity can greatly improve this situation. Nevertheless, it might appear that dynamical studies of molecules with many degrees of internal freedom could be tackled only with BD simulations. However, the presence of large potential barriers which hinder the conformational motions allows one to reduce the size of the matrix representation of the diffusion operator to the number of stable conformers. As mentioned above, a special set of functions, called localized functions, because they refer to equilibrium states of specific conformers, is suitable to generate the ME representation, by means of a projection procedure. Indeed, we do find that the ME method leads to a very rapid algorithm for the solution of these problems. Thus, the calculations described in this work take only 1–2 h of computer time. This great computational efficiency that we have been able to achieve clearly indicates the future potential in dealing with complex problems in molecular dynamics.

It should be stressed that the resulting ME is no longer a phenomenological equation but an asymptotic approximation to the starting equation with respect to the height of the potential barriers. Its range of validity is the same as that of the Kramers theory for activated processes, since it is implicitly assumed that the small amplitude motions inside the potential wells have a negligible effect on the long time behavior, determined mainly by the conformational transitions. Comparison with the complete solutions of one- and two-dimensional model systems shows that the ME method works nicely when the barrier heights are of the order of at least a few $k_B T$.[16] Therefore, when detailed potential surfaces are available, like those adopted in the BD simulations, they could be used to implement the ME method, and the results of the two techniques should be equivalent, except for the different degrees of accuracy noted below and for the validity of the asymptotic approximations.

Even though the ME method and BD simulations are based on the same diffusion equation, they should not be considered as alternative computational tools to be chosen simply according to their efficiency. They are, more correctly, complementary techniques providing information of a somewhat different nature. In principle, BD simulations provide a very detailed picture of the dynamical processes occurring in the system. In practice, however, the quality of the information obtained fades at long times. For example, the average kinetic rates for the $g_+ \rightarrow t$ and the $g_- \rightarrow t$ transitions at fixed positions of the chain, that should be identical for symmetry reasons, differ up to 45% in the calculations of Pastor *et al.* (see Table VIII of Ref. 3a), in spite of the very long computational time. The ME treatment renounces the description of the short time behavior of the system dynamics, focusing its attention on the relatively rare events of barrier crossings, i.e., to the kinetic regime of the conformational processes. Within the theoretical framework of the model, one can calculate very accurately the spectral densities, and so the multiexponential character of the decays to equilibrium can immediately be exhibited. In fact, it is these spectral densities that are needed in analyzing spin–relaxation data.

Furthermore, the ME method should be considered not only as a computational tool, but also as a theoretical method to gain more insight into the dynamical processes. For example, the calculation of the ensemble of the elementary transition rates entering in the master equation represents an intermediate step relating the molecular ingredients of the model (the potential and the friction matrix) to the physical observables of the system. The features of the model which are essential in determining the macroscopic behavior of the system, such as the potential curvature at the saddle points, or the frictional coupling between reactive and nonreactive modes that leads to a cooperative picture of single bond transitions, are easily recognized. This gives one the opportunity to select in the calculations only the relevant factors of the problem, and to disentangle the effects on the observables due to the various ingredients of the model, without having to deal with minor details. (Given that modern methods lead

to a very efficient algorithm for the ME approach, it becomes fairly easy to repeat calculations to test the effects of modifying various features of the model.) Previous work on alkyl chains in isotropic media have indeed shown that the ME approach allows a parametrization of the potential in terms of a few quantities with a direct physical meaning,[14] and substantial agreement has been found by comparison with NMR relaxation data.[17] We shall follow the same approach in treating the phospholipid chain dynamics in the membrane environment.

In Sec. II the RIS model applied to phospholipid chains is described. We also define there the time correlation functions for populations and for orientations that we calculate. Computational methods are discussed in Sec. III. Our results are discussed in Sec. IV. These include equilibrium properties such as order parameters and conformational populations, internal dynamical properties such as average isomerization rates and correlation functions of the angular variables, and also NMR relaxation. Our conclusions and comments appear in Sec. V. Therein we stress that the principal features of the results are determined by only a few microscopic parameters. Nevertheless, where comparisons with the BD calculations of Pastor–Venable–Karplus are appropriate, there is good agreement, and this strongly suggests that the ME approach is satisfactory, thereby providing simple physical insights into the nature of the internal configurational motions.

II. THE THEORETICAL MODEL

In Ref. 14 the time-dependent RIS model has been derived for an alkyl tail attached to a massive rigid core. We shall summarize here the main features of the model in order to illustrate its application to phospholipid chains in membranes. The structure of 1,2-dipalmitoyl-3-*sn*-phosphatidylcholine (DPPC), a typical membrane phospholipid, is represented in Fig. 1. As in the BD simulations of Pastor *et al.*,[3] we shall explicitly treat only chain 1. The carbon atoms of the chain are numbered from 1 to 16, starting from the carbonyl group. Since the torsional dynamics of the terminal methyl group will not be examined, the set $\alpha = (\alpha_1,\alpha_2,...,\alpha_{15})$ of 15 torsional angles represented in Fig. 1 is required to specify the conformational state of the chain.

As in the previous work,[14] we assume that conformational dynamics and overall motion are decoupled. In the case of isotropic liquids, this hypothesis relies on the different orders of magnitude of the friction opposing the overall rotation and opposing the conformational transitions.[18] This condition, however, is not necessarily sufficient in the present case, because of the coupling that results from the conformational dependence of the mean field potential for the anisotropic interactions of the test molecule with the membrane environment.

If we suppose that the position of the polar head is fixed with respect to the boundary of the bilayer, two independent contributions can be separated in the overall potential: the torsional potential V^{tors}, generated by the intramolecular interactions, and the mean-field potential V^{mf}, for the interactions of the chain with the environment

$$V = V^{\text{tors}}(\alpha) + V^{\text{mf}}(\alpha,\Omega). \tag{2.1}$$

In general, V^{mf} depends on both the chain conformation and the orientation Ω of the polar head with respect to the bilayer normal. It is possible to separate the potential into a conformational and an orientational term in the presence of very anisotropic interactions which strongly favor a given orientation Ω_0. (In the following treatment we shall assume the preferred orientation to be the one with the all-*trans* axis perpendicular to the bilayer surface.) More precisely, the potential V will be written as a sum of two terms: the internal contribution

$$V^{\text{int}}(\alpha) = V^{\text{tors}}(\alpha) + V^{\text{mf}}(\alpha,\Omega_0) \tag{2.2}$$

describing the potential acting on the molecule in the orientation Ω_0, and the external one

$$V^{\text{ext}}(\alpha,\Omega) = V^{\text{mf}}(\alpha,\Omega) - V^{\text{mf}}(\alpha,\Omega_0), \tag{2.3}$$

accounting for the increase of potential energy induced by fluctuations with respect to the preferred orientation. As long as V^{ext} is a steeply rising function of $\delta\Omega = \Omega - \Omega_0$, the weak dependence of V^{ext} on the torsional angles can be neglected. Therefore, the potential becomes factorized as

$$V(\alpha,\Omega) \cong V^{\text{int}}(\alpha) + V^{\text{ext}}(\Omega). \tag{2.4}$$

Note that this separation of variables is implicitly assumed whenever one factorizes the order parameter along the chain as a product of internal and external contributions.[19] Under the decoupling condition, the internal dynamics can also be treated independently of the overall rotational motion, as is usually done.[20,3]

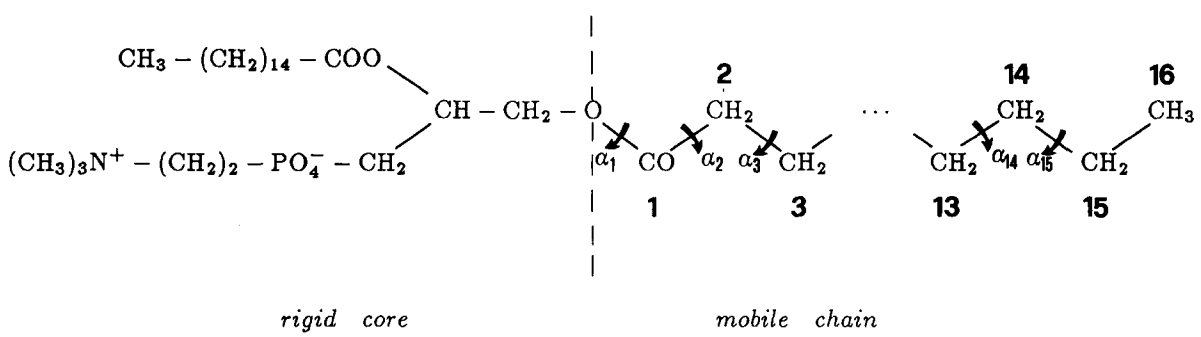

FIG. 1. Structure of the DPPC molecule.

If $f=f(\alpha)$ is a property depending on the 15 torsional variables α, its average value is calculated according to the RIS approximation[4] by means of the equation

$$\bar{f}=\sum_J f_J\, Q_J, \tag{2.5}$$

where J is an index denoting a stable configuration of the chain, $f_J \equiv f(\alpha^J)$ is the value of the function for the J th state, specified by the set α^J of torsional angles, and Q_J is the fractional population of the J th state, defined in terms of the "free energy" [21] E_J

$$Q_J=\frac{\exp(-E_J/k_BT)}{\sum_J \exp(-E_J/k_BT)} \tag{2.6}$$

with

$$E_J=V_J^{\text{int}}+\frac{kT}{2}\ln|\text{Det}(\mathbf{V}_J^{(2)}/2\pi k_BT)|. \tag{2.7}$$

In this expression V_J^{int} is the internal potential of the J th configuration, i.e., $V_J^{\text{int}}\equiv V^{\text{int}}(\alpha^J)$, and $\mathbf{V}_J^{(2)}$ the corresponding curvature matrix, i.e., the matrix of the second derivatives of the internal potential with respect to the torsional angles.

In Refs. 14, 15, and 17 the dynamics of the chain has been analyzed on the basis of a model assuming rotational diffusion around the bonds, by explicitly taking into account the coupling of the 15 torsional variables through both the potential and the frictional forces exerted by the surrounding viscous medium. By means of a projection procedure applied to the multivariate diffusion equation, a master equation is obtained for the time dependent conformer populations

$$\frac{\partial P_J(t)}{\partial t}=-\sum_{J'} W_{JJ'}\, P_{J'}(t). \tag{2.8}$$

If multiple bond transitions are neglected (because of their unfavorable activation energy[10]), then a parabolic expansion of the potential about the saddle points leads to the following form of off-diagonal elements of the transition matrix:

$$W_{JJ'}=-\frac{|\lambda_1|}{2\pi}\exp\left\{\frac{-(E_s-E_{J'})}{k_BT}\right\} \tag{2.9}$$

if the configuration J is reached from J' through a single rotation of a torsional angle, otherwise $W_{JJ'}$ is set equal to zero. In the above equation E_s is the free energy of the saddle point, calculated by analogy with Eq. (2.7) and λ_1 is the unique negative eigenvalue of the product matrix $\mathbf{D}_s\mathbf{V}_s^{(2)}/k_BT$, where $\mathbf{D}_s$ is the 15×15 diffusion matrix and $\mathbf{V}_s^{(2)}$ the curvature matrix, both calculated at the saddle point. The physical meaning of this procedure can easily be understood: the diagonalization of $\mathbf{D}_s\mathbf{V}_s^{(2)}$, appearing in the diffusion equation after a parabolic expansion, leads to the determination of 15 normal modes, but only one of them, corresponding to the negative eigenvalue λ_1, can be identified with the reaction coordinate, along which the transition rate is calculated.

The relation (2.9) holds for the off-diagonal elements of $\mathbf{W}$; the diagonal terms are calculated from the off-diagonal ones on the basis of the "detailed balance" condition

$$W_{JJ}=-Q_J^{-1}\sum_{J'\neq J} W_{JJ'}Q_{J'} \tag{2.10}$$

so that a stationary solution of Eq. (2.8) is given by the array $\mathbf{Q}$, having for elements the fractional populations Q_J.

Thus, static and dynamic properties can be calculated given the geometry and the energetics of the chain. In addition, a model is required to specify the frictional forces exerted by the environment.

A. Geometry of the chain

The chain geometry is characterized by fixed bond lengths and bond angles. The values are, respectively,[4,22] $l_{C_iC_{i+1}}=1.53$ Å, $C_{i-1}\hat{C}_iC_{i+1}=112°$, $H\hat{C}_iH=109°$.

By analogy with the central bond in the butane molecule, the rotation around the ith bond is assumed to be subjected to a torsional potential with three minima, respectively, at $\alpha_i=0°$ (*trans*) and $\alpha_i=\pm120°$ (*gauche*$_\pm$).[4,22,23] Then, according to the RIS approximation, a stable conformer can be identified by an ordered sequence of symbols specifying the conformational states of all the C–C bonds; e.g., the sequence ($tg_+g_-tt\cdots$) represents a configuration having the first bond in *trans*, the second in *gauche*$_+$, the third in *gauche*$_-$, and so on.

At the saddle points between two configurations, J and J', connected through a rotation about the ith bond, all of the nonreactive bonds are assumed to be in a stable conformational state (t,$g_\pm$), while the rotating segment is characterized by a value of the torsional angle α_i which is intermediate between the starting and the final one.

Moreover, the chain is described by an "extended atom" model. That is, each methylene group is described as a sphere with radius r_0, centered on the carbon atom.

B. Energetics of the chain

All the variables from α_3 to α_{15} are assumed to be subjected to the same butane-like torsional potential. The parametrization for the two remaining angles α_1 and α_2 is less straightforward; in agreement with Karplus and coworkers,[3] instead of a potential giving a realistic description of the rotational hindrance around these bonds, an effective one has been introduced, which reflects the contributions of the whole headgroup, and gives values of the equilibrium properties of the chain in agreement with the experimental data. The following parametrization has been used: α_1 is subjected to the usual butane-like torsional potential, while for α_2 the torsional potential has three equivalent minima at $\alpha_2=0°$ and $\pm120°$.

In summary, if the torsional potential of a *trans* and a *gauche* state is assumed to be 0 and V_g, respectively, the torsional contribution to the potential of the J th chain configuration can be written as

$$V_J^{\text{tors}}\equiv V^{\text{tors}}(\alpha^J)=n_gV_g, \tag{2.11}$$

where n_g is the number of *gauche* bonds in the chain, with the exclusion of the second bond.

Interactions among atoms separated by more than three bonds, which are not accounted for by the purely torsional potential, are considered at the level of excluded volume, i.e., by eliminating those configurations for which there is a superposition of the spheres representing the extended atoms. A given configuration is accepted only if the distance between any pair of carbon atoms separated by more than three bonds is larger than two extended atom radii. We have chosen $r_0 = 1.85$ Å, a value which agrees with the van der Waals radius of the extended atoms assumed in trajectory simulations of hydrocarbon chains.[2,3] In this way, all the configurations containing adjacent *gauche* states are excluded. This may be too restrictive a choice for free chains, because it strongly reduces the number of available configurations. However, it seems to be adequate to represent phospholipid tails in a membrane environment, because it makes the folded configurations by far less probable than the extended ones. Note that, because of the exclusion of adjacent *gauche* states the so-called "pentane effect" does not need to be explicitly considered. The effect of the bilayer surface is taken into account by eliminating configurations with part of the chain bent behind a plane passing through C_1 and orthogonal to the all-*trans* axis. With these choices, the number of allowed configurations is reduced from $3^{15} = 14\,348\,907$ to 37 225.

The orienting effect of the bilayer environment on the chain has been described by a mean-field external potential, which depends on the conformation. According to the treatment of phospholipid chains by Marcelja[24] and that of flexible mesogens in nematic phases by Emsley, Luckhurst, and Stockley,[25] the dispersive interactions of the chain with the environment are described by a mean field potential given by a sum of contributions, each relative to a segment. The pseudopotential acting on the J th configuration is written as

$$V_J^{\mathrm{mf}} = -\epsilon \sum_{i=1}^{15} P_2(\cos\beta_{\mathrm{HCH}}^{i}), \tag{2.12}$$

where ϵ is a parameter giving the strength of the potential, P_2 is the second Legendre polynomial, and β_{HCH}^{i} is the angle between the normal to the HC_iH plane and the all-*trans* axis.[26]

In addition, in order to calculate static and dynamic properties of the chain, knowledge of the curvature matrices in the stable configurations $\mathbf{V}_J^{(2)}$ and at the saddle points $\mathbf{V}_s^{(2)}$ is required. In principle, the curvatures can be obtained from the analytical form of the internal potential; however, we have adopted a simpler parametrization procedure. Both matrices are assumed to be diagonal with respect to the displacements of the torsional angles α_i. In particular, in the stable configurations there is a unique positive curvature $V_{\mathrm{nr}}^{(2)}$ so that $\mathbf{V}^{(2)} = \mathbf{1}V_{\mathrm{nr}}^{(2)}$. The same positive curvature $V_{\mathrm{nr}}^{(2)}$ characterizes the nonreactive bonds at the saddle points, while a negative curvature $V_r^{(2)}$ is associated with the "reactive mode" α_k modified by the single bond transition.

The free energy of the saddle points is calculated by assuming that each of them is characterized by the same increase ΔE_s with respect to the highest value at the two connected configurations; that is, the energy at the saddle point for a transition $J \rightarrow J'$ is given by

$$E_s = \max(E_J, E_{J'}) + \Delta E_s. \tag{2.13}$$

C. Hydrodynamics

The diffusion tensor $\mathbf{D}_s$ is written as $kT(\tilde{\boldsymbol{\xi}}^s)^{-1}$, and the friction matrix $\tilde{\boldsymbol{\xi}}^s$ is calculated by hydrodynamical methods. The torsional degrees of freedom are assumed to be uncoupled to the overall rotation of the molecule because of the strong forces acting on the headgroups of the phospholipid chain. The rotation about the C_{k-1}–C_k bond causes translations of all the spheres following the k th one, and the elements of the friction matrix can be calculated as[14,15]

$$\xi_{ki}^{s} = \xi_0 \sum_{m=m'}^{16} [\mathbf{z}_{k-1} \times (\mathbf{r}_m - \mathbf{r}_k)] \cdot [\mathbf{z}_{i-1} \times (\mathbf{r}_m - \mathbf{r}_i)], \tag{2.14}$$

where m' is the larger of the integers $(k+1)$ and $(i+1)$, ξ_0 is the friction opposing the translational motion of a single sphere, $\mathbf{z}_{k-1}$ is a unit vector along the $C_{k-1} - C_k$ bond, and $\mathbf{r}_m$ the position vector of the mth carbon atom.

D. Dynamical properties

A given bond is characterized by a variety of $g \rightarrow t$ and $t \rightarrow g$ transition rates, depending on the conformation of all the other bonds. However, the dynamical results can be rationalized in terms of average isomerization constants. The average kinetic rate for the $g_{\pm} \rightarrow t$ transitions of the ith bond is defined as[15]

$$\overline{k_{g \rightarrow t}^{i}} = \sum_{JJ'}^{*} W_{JJ'} Q_{J'} \Big/ \sum_{J}^{*} Q_J, \tag{2.15}$$

where the asterisk denotes that only transition matrix elements between states connected by a $g_{\pm} \rightarrow t$ conformational change at the ith chain segment are retained in the summation. The average rate constant $\overline{k_{t \rightarrow g}^{i}}$ is defined in an analogous way.

Alternatively, the dynamics can be analyzed by means of some relevant correlation functions. Given the function $f = f(\alpha)$, the correlation function for its deviation from the equilibrium average is defined as

$$F(t) = \overline{\delta f^{\dagger}(t)\delta f(0)} = \delta \mathbf{f}^{\dagger} e^{-\mathbf{W}t} \mathbf{S} \delta \mathbf{f}. \tag{2.16}$$

In this expression $\mathbf{S}$ is a diagonal matrix with elements $S_{JJ} = Q_J$, and $\delta\mathbf{f}$ is a vector whose J th element

$$(\delta f)_J = f_J - \bar{f} \tag{2.17}$$

is the deviation of the value of the function for the J th configuration from its mean value. Actually, instead of the correlation functions, the corresponding spectral densities, i.e., their Fourier–Laplace transforms, are calculated by the following expression:

$$\tilde{F}(\omega) = \delta \mathbf{f}^{\dagger} (i\omega \mathbf{1} + \mathbf{W})^{-1} \mathbf{S} \delta \mathbf{f}. \tag{2.18}$$

In particular, it is possible to define effective decay rates as the inverse of the properly normalized time integrals of the correlation functions

$$K = F(0)/\tilde{F}(0). \tag{2.19}$$

We have considered two different kinds of functions, population functions and angular functions. The first group in-

cludes functions describing the excess of *trans* population and the unbalanced *gauche* population at a given site; the components of the corresponding vectors are defined as

$$(\mathscr{P}_t^i)_J = \delta_{J_i,t} \tag{2.20a}$$

and

$$(\mathscr{P}_g^i)_J = \delta_{J_i,g_+} - \delta_{J_i,g_-}, \tag{2.20b}$$

where J_i gives the conformation of the ith bond in the Jth state. In the case of a molecule with one internal degree of freedom, the decay constants for these functions can be related to the rate constants associated with the $g \rightarrow t$ and the $t \rightarrow g$ processes, $k_{g\rightarrow t}$ and $k_{t\rightarrow g}$. In this case $\delta\mathscr{P}_t$ and $\delta\mathscr{P}_g$ are eigenvectors of the transition matrix, corresponding respectively to the eigenvalues

$$\begin{aligned} K_t &= k_{g\rightarrow t} + 2k_{t\rightarrow g}, \\ K_g &= k_{g\rightarrow t}. \end{aligned} \tag{2.21}$$

In fact, it turns out that, if the rate constants in Eq. (2.21) are replaced with the average kinetic rates defined by Eq. (2.15), analogous relationships are approximately satisfied for more complex chains despite the couplings deriving from the configuration-dependent friction, the excluded volume interactions, and the mean field potential, provided that they are not too strong.[14]

The angular functions we have considered are $D^2_{m0}(\Omega_{\mathrm{mol},F_i})$, components of Wigner rotation matrices of rank 2 having for argument the Euler angles for the transformation mol$\rightarrow F_i$, where F_i is a local frame, centered on the ith carbon, with the z axis along a C_i–H bond. The conformation-independent molecular frame denoted by mol is centered on the acylic oxygen at the fixed end of the chain, with the Z axis along the all-*trans* direction, and the X axis in the plane bisecting the $\widehat{HC_iH}$ angles in the all-*trans* conformation.

These functions have been chosen because of their physical meaning, since they are the suitable functions to describe the time evolution of axially symmetric tensors of rank two with the symmetry axis along the C_i–H bonds; (examples of interest in the case of hydrocarbon chains are the magnetic interaction tensors in ^{2}H and ^{13}C NMR experiments). Actually, the experimental observables can be expressed in terms of the Wigner functions $D^2_{p0}(\Omega_{\mathrm{lab},F_i})$, with $\Omega_{\mathrm{lab},F_i}$ the Euler angles relating the principal axes of the tensorial interactions to the laboratory frame, chosen according to the conventions of Rose.[27] By making use of the addition theorem for the Wigner functions, these functions can be factorized as

$$D^2_{p0}(\Omega_{\mathrm{lab},F_i}) = \sum_{m=-2}^{2} D^2_{pm}(\Omega_{\mathrm{lab,mol}}) D^2_{m0}(\Omega_{\mathrm{mol},F_i}), \tag{2.22}$$

where $\Omega_{\mathrm{lab,mol}}$ represents the Euler rotations, from the laboratory to the molecular frame. Then given (1) the hypothesis of decoupling of internal and overall motion, (2) the average lipid conformation is axially symmetric about the all-*trans* axis, (3) that the external potential V^{ext} is only a function of the angle β between this axis and the director, and (4) that the overall motion is also axially symmetric, the correlation function $G^i_p(t)$, for the deviation of $D^2_{p0}(\Omega_{\mathrm{lab},F_i})$ from its average value, can be decomposed as[14]

$$\begin{aligned} G^i_p(t) = \sum_m \{ & C_{pm}(t)[g^i_m(t) + |S^i_m|^2] \\ & + \delta_{m,0}\delta_{p,0} S^2_0 g^i_0(t)\}. \end{aligned} \tag{2.23}$$

In Eq. (2.23), $g^i_m(t)$ and $C_{pm}(t)$ are the correlation functions, respectively, for the deviations of $D^2_{m0}(\Omega_{\mathrm{mol},F_i})$ and $D^2_{pm}(\Omega_{\mathrm{lab,mol}})$ from their equilibrium values, denoted by S^i_m and by S_0. [Given our assumptions, only the average value of $D^2_{00}(\Omega_{\mathrm{lab,mol}})$ is different from zero.]

III. COMPUTATIONAL METHODS

The computations have been performed on an IBM 3090 supercomputer at the Cornell National Supercomputer Facility, according to the following scheme:

(1) generation of the allowed conformations and calculation of the equilibrium averages;

(2) calculation of the transition matrix;

(3) for each relevant function, calculation of the corresponding vector δf and of the spectral density through the Lanczos Algorithm.

We now consider these steps.

(1) All possible configurations are generated. The configurations are examined and the sterically hindered ones are rejected according to the criteria introduced above. Also a check must be performed in order to eliminate all the configurations which cannot be connected with the all-*trans* by a sequence of single bond transitions. This is because there would be problems in the calculation of the dynamic properties without this check, due to slightly nonergodic features for finite times. It is important to note that this operation does not introduce artificial effects because of the small number of "bad" configurations (only 44) and their low statistical weight (0.002% on the partition function). The final number of retained configurations is 37 181 (N_c).

At this step of the computation, fractional populations of the stables states and equilibrium properties, given, respectively, by Eqs. (2.6) and (2.5), are evaluated.

(2) Because of the convenience of working with symmetric operators, the transition matrix is used in its symmetrized form $\widetilde{\mathbf{W}}$ whose elements are defined as

$$\widetilde{W}_{JJ'} = Q_J^{-1/2} W_{JJ'} Q_{J'}^{1/2}. \tag{3.1}$$

By using the parametrization suggested in Sec. II B, the matrix elements can be expressed as

$$\widetilde{W}_{JJ'} = -\frac{w}{|\mu_1|} \exp\left\{ -\frac{|E_J - E_{J'}|}{2k_B T} \right\}, \tag{3.2}$$

where μ_1 is the unique negative eigenvalue of the matrix

$$\mathbf{M} = (\mathbf{V}_s^{(2)-1} |V_r^{(2)}|) \tilde{\xi}^s / \xi_0 l^2_{CC}. \tag{3.3}$$

Because of the $|V_r^{(2)}|$ scaling of the $\mathbf{V}_s^{(2)}$ matrix, only the knowledge of the ratio ρ of the curvatures for the reactive and the nonreactive modes

$$\rho = \frac{|V_r^{(2)}|}{V_{nr}^{(2)}} \tag{3.4}$$

is required, instead of their absolute values. The parameter w appearing in Eq. (3.2) is defined as

$$w = \frac{V_r^{(2)}}{2\pi l_{CC}^2 \xi_0} \exp\left\{ -\frac{\Delta E_s}{k_B T} \right\}. \quad (3.5)$$

If the free energy increment ΔE_s is assumed to be the same as for the butane molecule, w has an immediate physical meaning, corresponding, apart from a geometrical factor, to the butane $g \rightarrow t$ isomerization rate.

The calculation of the transition matrix $\tilde{\mathbf{W}}$ for the 15-bond chain is a difficult job, because of the time and space requirements. In principle, N_c^2 elements should be computed and stored; fortunately, this number can be noticeably reduced, if use is made of the properties of the matrix, in particular, of its sparsity. Actually, only a small fraction of states (a number less than 30, in this case) are connected with a given configuration by single bond transitions; direct conversion between *gauche* states is not allowed, because of the high energy barrier[4] for all bonds with the exception of the second, for which, as a consequence of the threefold symmetric potential, any rotation of $\pm 120°$ is possible.

For each off-diagonal nonzero element the scaled friction matrix $\tilde{\xi}^s/\xi_0 l_{CC}^2$ is calculated; then the 15×15 real nonsymmetric $\mathbf{M}$ matrix defined in Eq. (3.3) has to be diagonalized in order to obtain the negative eigenvalue μ_1. These tasks are efficiently accomplished by properly implementing Eq. (2.14) and by using the diagonalizing subroutine RG of the EISPACK package.[28]

At this stage of the calculation, with a very little additional computational effort, it is possible to obtain the average isomerization rate constants, defined by Eq. (2.15).

In conclusion, the computation of the matrix required about an hour of CPU time.

(3) Given the sparsity of the matrix $\tilde{\mathbf{W}}$ it is natural to calculate the correlation functions and spectral densities by the Lanczos algorithm[29–31] (LA), which allows the storage of the nonzero elements only. Two kinds of correlation function have been calculated, angular correlation functions and population correlation functions. For each correlation function, the starting vector was calculated according to Eq. (2.17); for both kinds of functions this step required less than 30 s of CPU time.

By applying the LA to the real symmetric matrix $\tilde{\mathbf{W}}$ with the different starting vectors corresponding to the various correlation functions, continued fractions were generated, which were stored and analyzed. The LA proved to be very efficient: in general, the zero frequency spectral densities calculated from the continued fractions converged at least to the fourth significant figure after about 45 steps. The time taken for 200 steps of the Lanczos algorithm was of the order of 2 min. To fully apreciate the efficiency of the method, it should be remembered that at least five correlation functions must be calculated for each segment [i.e., the three independent $D^2_{m0}(\Omega_{\mathrm{mol},F_i})$ and the two $\mathcal{P}_t^i$ and $\mathcal{P}_g^i$], and the time required by the Lanczos procedure (proportional to $15 \times N_c \times n_L$, where n_L is the number of LA steps) should be compared with the time for conventional diagonalization techniques, which in this case would have been of the order of N_c^3.

IV. RESULTS

A. Equilibrium properties

In this subsection distributions of conformational states along the chain and some static properties directly related to experimental measurements, such as the order parameters will be discussed. Calculations have been performed with the energy parameters $v_g = V_g/k_B T = 0.84$ and $\epsilon^* = \epsilon/k_B T = 0.3$; the first corresponds to a *trans–gauche* energy difference of 500 cal/mol[4], and the second agrees with the value used by Emsley *et al.*[25] for liquid crystals.

The parameter ρ has been chosen equal to 1, while w does not need to be specified, since all the dynamical quantities are given in units of w; (in order to compare the calculated quantities with experimental ones, we will later assume w to be of the order of [32] 10^{10} rad s^{-1}). The values used for the geometric parameters have already been specified.

With the chosen value of r_0, no more than eight bonds in the chain can be in a *gauche* state. In addition, the extended configurations are favored by the *gauche–trans* energy difference and by the external orienting potential. As a consequence, it turns out that, on the average, more than eleven bonds are in a *trans* state.

Figure 2 shows P_t^i, the probability of finding a *trans* at the ith bond, and P_{kink}^i, the probability, for the ith segment, of being the center of a kink ($g_\pm tg_\mp$); (note that P_{kink}^i is scaled by 10). Values of other quantities related to average conformations are given in Table I. The *trans* bonds are shown in Fig. 2 to be distributed rather homogeneously along the chain, with a slight odd–even effect, particularly evident near the head of the chain. (To compare, note that the value of P_t^i for the butane molecule, with the same torsional potential assumed in this calculation, would be 0.53.) By analogy to P_t^i, P_{kink}^i also shows a plateau over all the internal bonds. The exceptionally high value at the third bond is probably an artificial effect, introduced as a consequence of the shape chosen for the torsional potentials at the first two bonds. However, the important result is that the probability of being the center of a kink is an order of magnitude lower than the probability of a *trans* in any position. This result, together with the fact that the fraction of config-

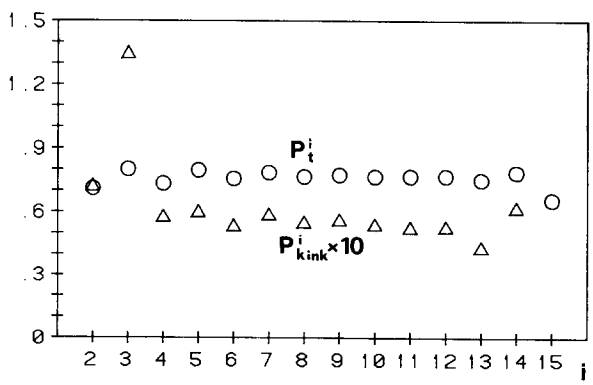

FIG. 2. Plots of P_t^i (circles) and P_{kink}^i (triangles), probability of finding respectively a *trans* state and the center of a kink at the ith bond. P_{kink}^i is scaled by 10.

TABLE I. Equilibrium conformational distributions and chain distances.

[a]	$\overline{C}_t$	0.764
[b]	P_{kink}	0.117
[c]	P'_{kink}	0.571
[d]	$\overline{Z}_{16}$	13.76 Å
[e]	$\overline{Z}_{15}$	13.14 Å
[f]	$Z_{16\,\text{a.t.}}$	19.03 Å
[g]	$Z_{15\,\text{a.t.}}$	17.76 Å

[a] Average concentration of *trans* bonds in the chain.
[b] Global probability of configurations containing only kinks.
[c] Global probability of configurations containing only kinks, in addition to other $g_\pm$ conformations.
[d] Average distance C_1–C_{16}.
[e] Average distance C_1–C_{15}.
[f] Distance C_1–C_{16} in the all-*trans* configuration.
[g] Distance C_1–C_{15} in the all-*trans* configuration.

urations containing only kinks is less than 12% of the total (see Table I), clearly shows the inadequacy of a model considering only kinks,[12,13] at least for calculating the static properties.

In Table II, the deuterium order parameter S^i_{CD} and the segmental order parameter S^i_C are listed for the various positions in the chain. They are defined as

$$S^i_{CD} = \overline{P_2(\cos\beta^i_{CD})} \tag{4.1}$$

and

$$S^i_C = \overline{P_2(\cos\beta^i_{HCH})}, \tag{4.2}$$

i.e., they are the average values of the second Legendre polynomials having for argument the cosine of the angles formed by the C_i–D bond (β^i_{CD}), [or by the perpendicular to the $\widehat{HC_iH}$ angle (β^i_{HCH})], with the all-*trans* axis. In a rigid chain it would be $S^i_{CD} = -0.5$ and $S^i_C = 1.0$, and in general, for an isotropic distribution of the polar angle defining the orientation of the all-*trans* axis in the local frame F_i, the two parameters are related by

$$S^i_{CD} = -S^i_C/2. \tag{4.3}$$

Such an isotropic distribution is not actually required by symmetry considerations in the aliphatic chains, and in fact, the calculated order parameters deviate slightly from the values predicted by Eq. (4.3), as reported in Table II. It is interesting to note that a similar result is also reached in MD simulations,[2] despite the fact that the allowed fluctuations of the bond angles are expected to randomize more effectively the orientational distributions of the bond vectors.

Because of the mean field potential described by Eq. (2.12), the absolute values of both order parameters show the following typical behavior. There is a plateau for the first part of the chain, followed by a series of more rapidly decreasing values. It is interesting to compare these data with those for P^i_t. Although the fraction of *trans* states at a given site, which is a strictly local property, remains approximately the same for all bonds but the extreme ones, the order parameters decrease continuously, because they depend on the conformational freedom, not only of the segment to which they refer, but also of all the previous bonds along the chain. A slight odd–even effect, more pronounced near the fixed end of the chain, can be observed for both S^i_{CD} and S^i_C.

The quantities S^i_{CD} can be compared with the observed order parameters derived from the quadrupolar splittings in ^{2}H NMR spectra[33,34] and those obtained from the dipolar splittings of ^{13}C NMR spectra,[35] while the order parameters derived from ESR spectra[36,37] are functions of S^i_C, and those obtained from proton NMR[38] can be expressed in terms of S^i_C and S^i_{CD}.

The behavior predicted by the calculations agrees, at least from a qualitative point of view, with the experimental results. To perform a quantitative comparison, one must remember that the experimental quantities are determined not only by the internal motions, but also by the overall rotations of the molecule, which contribute to change the mean orientation of a given bond of the chain. If overall and internal dynamics can be assumed to be uncoupled, and the average lipid conformation is axially symmetric about the all-*trans* axis, the following relationship holds for the experimental order parameter[19] S'^i_{CD}:

$$S'^i_{CD} = S_0|S^i_{CD}|, \tag{4.4}$$

where S_0 is an order parameter for the all-*trans* axis. Because of Eq. (4.4), all the calculated S^i_{CD} have to be rescaled in order to be compared with the experimental data. As an illustration, in Fig. 3 the scaled order parameters, obtained

TABLE II. Calculated C–D bond and segmental order parameters.

i	S^i_{CD}	S^i_C
2	−0.288	0.523
3	−0.273	0.488
4	−0.295	0.539
5	−0.290	0.533
6	−0.292	0.539
7	−0.280	0.517
8	−0.275	0.508
9	−0.263	0.484
10	−0.256	0.470
11	−0.242	0.443
12	−0.232	0.423
13	−0.213	0.385
14	−0.195	0.350
15	−0.149	0.259

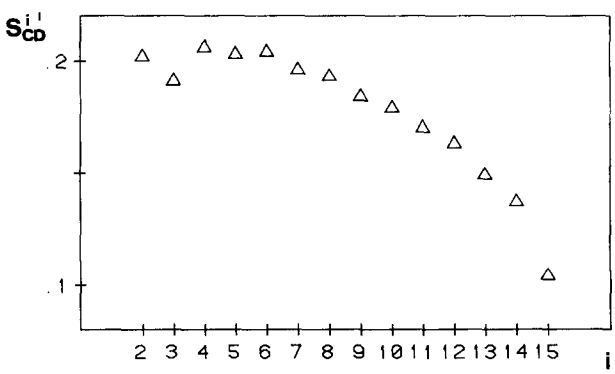

FIG. 3. Scaled order parameters S'^i_{CD} obtained with $S_0 = 0.7$.

assuming for S_0 the reasonable value of 0.7,[19b,3] are plotted as a function of the position in the chain.

Other interesting quantities related to the rigidity of the chain are the mean projections of the positions of the carbons on the all-*trans* axis $\overline{Z_i}$. For the present model, the mean chain length calculated from the carbon C_1, $\overline{Z_{16}}$, is 13.76 Å, which can be compared with the value for the extended chain, that is 19.03 Å. The BD simulations of Pastor *et al.*[32] give a value of 11.68 Å for the average position of C_{15} along the bilayer normal ($Z_{15}^{\perp}$), in agreement with neutron scattering data.[39] This datum can be related to the calculated $\overline{Z_{15}}$ by means of the relation

$$\overline{Z_{15}^{\perp}} = \overline{Z_{15}} \cdot \overline{\cos\theta}, \tag{4.5}$$

where θ is the angle between the all-*trans* axis and the bilayer normal, which can change because of the overall motion of the molecule. For small angles the power series expansion of the cosine function can be truncated at the second term and the following expression holds:

$$\overline{Z_{15}^{\perp}} \approx \overline{Z_{15}} \frac{2+S_0}{3}. \tag{4.6}$$

With $S_0 = 0.7$ a value of 0.9 is obtained for $\overline{\cos\theta}$, and, after multiplication by the theoretical result $\overline{Z_{15}} = 13.14$ Å, a value of 11.83 Å for $\overline{Z_{15}^{\perp}}$ is computed.

B. Dynamical properties

The internal dynamics of the chain is reflected by the average isomerization rates, calculated for the various segments according to Eq. (2.15). In Fig. 4 $\log \overline{k_{g\to t}^i}$ (triangles) and $\log \overline{k_{t\to g}^i}$ (circles) are shown for the various positions in the chain. Both isomerization rates show typical plateau values for the central bonds, which is a consequence of the expected cooperativity of the motions, explicitly taken into account by the dynamical model. The degree of cooperativity depends on the shape of the potential $V^{\text{int}}(\alpha)$, in particular, on its curvatures with respect to the torsional variables, which, with the present parametrization, is accounted for by the ratio ρ. A zero value of this parameter would imply sharp minima and flat maxima, so that a given rotation cannot be assisted by rearrangements around the other bonds; in this situation, where the segments are only coupled by frictional effects, both kinds of rate constants are increasing functions of the chain position, as a consequence of the decreasing friction. This behavior was already analyzed in detail in a series of calculations of the average rate constants by a Monte Carlo procedure.[15] By comparing with those results, obtained for the case of an isotropic medium, the important point emerges that, in contrast to the static properties, the rate constants are only weakly affected by an orienting potential. This agrees with the results obtained by Pastor *et al.*[3] in their BD simulations.

In Fig. 5, the rate constants $\overline{k_{g\to t}^i}$ are plotted together with the decay rates, K_t^i and K_g^i of the functions describing, respectively, the excess of *trans* population and the unbalanced *gauche* population at a given site. The relations (2.21) between the rate constants K_t^i and K_g^i and the average isomerization constants $\overline{k_{g\to t}^i}$ and $\overline{k_{t\to g}^i}$ are no longer necessarily meaningful here because of the strong couplings among segments. On the other hand, it appears that in any segment the values of both decay rates (in particular, K_g^i) follow rather closely those of the kinetic constant for the $g_{\pm} \to t$ transitions.

A completely different behavior is found for the decay constants for the angular functions. Here the functions $D_{m0}^2(\Omega_{\text{mol},F_i})$, (components of Wigner rotation matrices of rank 2 having for argument the Euler angles for the transformation mol$\to F_i$), are considered. In Fig. 6, the constants K_m^i defined for the different components ($m = 0,1,2$) by expressions analogous to Eq. (2.19) are plotted for the various positions. All these constants show a similar behavior, different from that of the $\overline{k_{g\to t}^i}$. In particular, they do not show any plateau. This result is particularly evident in the logarithmic plot displayed in Fig. 7, where the kinetic constants $\overline{k_{g\to t}^i}$ are compared with the average decay constants for the Wigner components K^i defined as

$$K^i = \left[\sum_{m=-2}^{2} (K_m^i)^{-1} g_m^i(0) \Big/ \sum_{m=-2}^{2} g_m^i(0) \right]^{-1}. \tag{4.7}$$

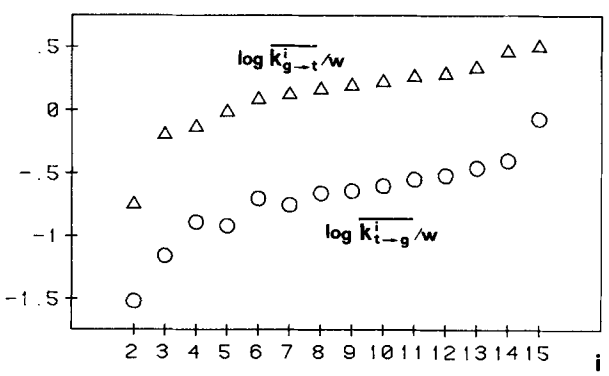

FIG. 4. Logarithmic plot of the average kinetic constants $\overline{k_{g\to t}^i}$ (triangles) and $\overline{k_{t\to g}^i}$ (circles).

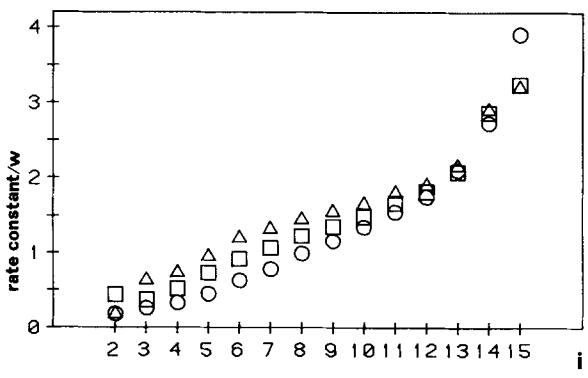

FIG. 5. Comparison of the average kinetic constants $\overline{k_{g\to t}^i}$ (triangles) with the decay rates for the unbalanced *gauche* population K_g^i (squares) and the *trans* population K_t^i (circles) at a given site.

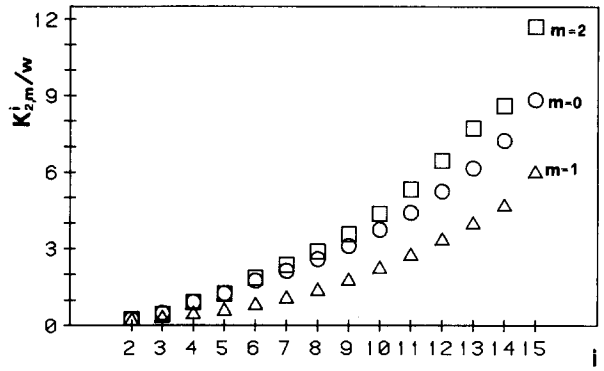

FIG. 6. Decay constants K^i_m of the components of the Wigner rotation matrices $D^2_{m0}(\Omega_{\mathrm{mol},F_i})$ with $m=0$ (circles), $m=1$ (triangles), and $m=2$ (squares).

As already discussed in relation to the static properties, the reason is to be found in the fact that these rate constants are not just related to local properties, since the time evolution of a given $D^2_{m0}(\Omega_{\mathrm{mol},F_i})$ is determined not only by the dynamics of the ith bond, but also by the motions of all the previous bonds in the chain.

It is also interesting to look at the full spectral densities of the angular functions, to obtain information on the spread of the decay times. For this purpose the Cole–Cole[14] plots of the spectral densities for functions located at positions C_4, C_8, and C_{15} in the chain are shown in Fig. 8. In all cases there are large deviations from monoexponentiality, particularly for the components $D^2_{10}(\Omega_{\mathrm{mol},F_i})$.

In Table III the squares of the equilibrium averages of the functions $D^2_{m0}(\Omega_{\mathrm{mol},F_i})$ and the mean square values of their deviations from equilibrium (i.e., the initial time values of the corresponding autocorrelation functions) are given for the different C_i–D bonds in the chain; they can be compared with the values for an isotropic distribution, which are 0 and 1/5, respectively.

C. NMR relaxation

It is tempting to relate the results of the dynamic model to those experiments sensitive to the mobility of the different

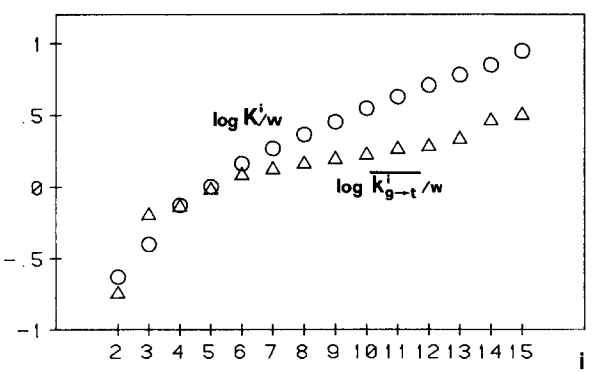

FIG. 7. Logarithmic plot of the kinetic constants $\overline{k^i_{g-t}}$ (triangles) and the average decay constants for Wigner components K^i (circles).

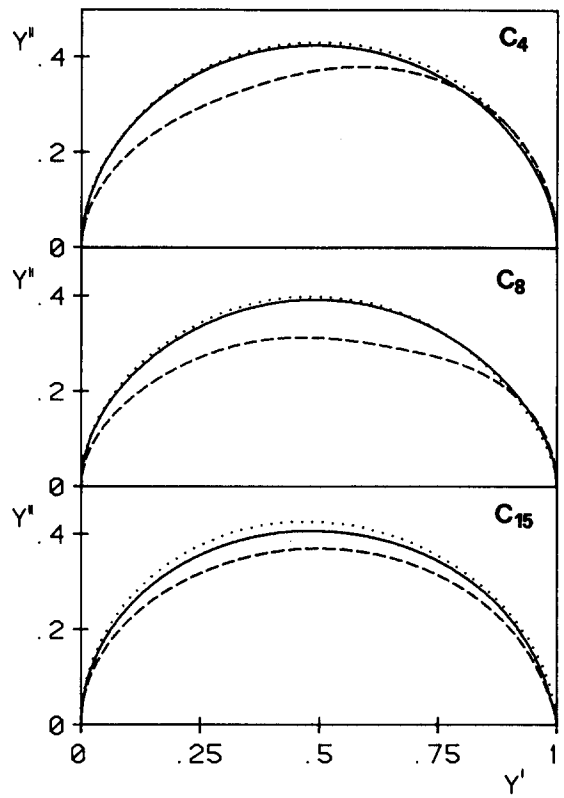

FIG. 8. Cole–Cole plots of the normalized spectral densities, $Y=j^i_m(\omega)/j^i_m(0)$, for C_4, C_8, and C_{15} (— $m=0$, --- $m=1$, $\cdots$ $m=2$).

segments in the chain. Examples of such experiments, from which many interesting data have been derived, are measurements of the NMR T_1 and T_2 relaxation times, especially for ^{13}C and ^2H. Unfortunately, the interpretation of the experimental data is not straightforward, even if a model for the internal motions is available, because the results depend not only on the internal dynamics, but also on other motional processes, including overall orientational diffusion of the chain, collective fluctuations, and lateral diffusion that could induce reorientations of the chain axis. Because of un-

TABLE III. Squares of the equilibrium averages of the Wigner components $D^2_{m0}(\Omega_{\mathrm{mol},F_i})$ and mean square values of their deviations from equilibrium.

i	$\lvert\overline{D^2_{00}}\rvert^2$	$\lvert\overline{D^2_{10}}\rvert^2$	$\lvert\overline{D^2_{20}}\rvert^2$	$\lvert\overline{\delta D^2_{00}}\rvert^2$	$\lvert\overline{\delta D^2_{10}}\rvert^2$	$\lvert\overline{\delta D^2_{20}}\rvert^2$
2	0.083	0.002	0.050	0.157	0.075	0.253
3	0.075	0.001	0.038	0.165	0.082	0.259
4	0.087	0.000	0.057	0.154	0.074	0.248
5	0.084	0.000	0.057	0.157	0.076	0.246
6	0.085	0.000	0.061	0.157	0.075	0.243
7	0.078	0.000	0.054	0.163	0.079	0.246
8	0.076	0.000	0.053	0.166	0.080	0.246
9	0.069	0.000	0.047	0.173	0.084	0.247
10	0.066	0.000	0.046	0.177	0.086	0.246
11	0.059	0.000	0.041	0.183	0.091	0.247
12	0.054	0.000	0.037	0.189	0.094	0.247
13	0.045	0.000	0.029	0.198	0.100	0.249
14	0.038	0.000	0.022	0.205	0.106	0.250
15	0.022	0.001	0.008	0.220	0.121	0.248

certainties in the theoretical estimate of the role of the two latter processes, only the overall motion of the chain will be explicitly considered in the following.

The NMR relaxation frequencies for a quadrupolar interaction tensor axially symmetric along a C_i–D bond are given by[40]

$$(T_1^i)^{-1} = \frac{3}{8}\left(\frac{e^2qQ}{h}\right)^2 [\mathcal{J}_1^i(\omega_D) + 4\mathcal{J}_2^i(2\omega_D)] \tag{4.8}$$

and

$$(T_2^i)^{-1} = \frac{1}{16}\left(\frac{e^2qQ}{h}\right)^2 \times [9\mathcal{J}_0^i(0) + 15\mathcal{J}_1^i(\omega_D) + 6\mathcal{J}_2^i(2\omega_D)], \tag{4.9}$$

where e^2qQ is the quadrupole coupling constant, ω_D the Larmor frequency of the ^{2}H nucleus, and $\mathcal{J}_l^i$ is the spectral density for the deviation from the equilibrium value of the Wigner rotation function $D_{l0}^2(\Omega_{\text{lab},F_i})$, for Ω_{lab,F_i} the Euler angles relating the principal axis system of the magnetic interaction tensor to the laboratory frame [cf. Eq. (2.22)], where the Z axis is parallel to the static magnetic field. In place of Eq. (2.22) we shall introduce a more general factorization of $D_{l0}^2(\Omega_{\text{lab},F_i})$

$$D_{l0}^2(\Omega_{\text{lab},F_i}) = \sum_{p,m=-2}^{2} D_{lp}^2(\Omega_{\text{lab},n}) D_{pm}^2(\Omega_{n,\text{mol}}) \times D_{m0}^2(\Omega_{\text{mol},F_i}), \tag{4.10}$$

where $\Omega_{\text{lab},n}$, $\Omega_{n,\text{mol}}$, and Ω_{mol,F_i} represent, respectively, Euler rotations from the laboratory system to a frame having the Z axis parallel to the director, from the director frame to the molecular one, and from this frame to the local frame diagonalizing the magnetic interaction tensor. Then, it is possible to write

$$\mathcal{J}_l^i = \sum_{p=-2}^{2} [d_{lp}^2(\beta_{\text{lab},n})]^2 J_p^i, \tag{4.11}$$

where J_p^i is the spectral density associated with the correlation function G_p^i introduced in Eq. (2.23). In order to calculate these quantities, a model for the overall rotation has to be introduced. This motion can be described as restricted diffusion in a uniaxial potential field which tends to align the long molecular axis to the normal to the bilayer. The potential V^{ext} has been chosen according to the Maier–Saupe theory.[41,42] The diffusion tensor is assumed to be independent of the conformation of the chain; (which can be justified because the aliphatic tail is attached to a massive core, the polar head and the other chain[18]), and is axially symmetric, with the symmetry axis along the all-*trans* direction. Following standard procedures, the autocorrelation function $C_{pm}(t)$ may be calculated by expanding the diffusion operator in a basis of orthogonal functions.[41,42] Here we shall use a simpler approach, which leads to a single-exponential expression. Because of independence of the mean field potential on the Euler angles $\alpha_{n,\text{mol}}$ and $\gamma_{n,\text{mol}}$, it is possible to write

$$C_{pm}(t) = c_{pm}(t)\exp[-(D_\parallel - D_\perp)m^2 t], \tag{4.12}$$

where c_{pm} is a reduced correlation function depending only on the variable $\beta_{n,\text{mol}}$, for which a single-exponential approximation has been found to be a satisfactory one[20,43]

$$c_{pm}(t) = a_{pm}\exp(-t/\tau_{pm}). \tag{4.13}$$

In this expression

$$a_{pm} = \overline{[\delta d_{pm}^2(\beta_{n,\text{mol}})]^2}, \tag{4.14}$$

where $\delta d_{pm}^2(\beta_{n,\text{mol}})$ is defined as the deviation of the function $d_{pm}^2(\beta_{n,\text{mol}})$ from its equilibrium value $\overline{d_{pm}^2(\beta_{n,\text{mol}})}$, and

$$\tau_{pm}^{-1} = \langle \delta d_{pm}^2 | \hat{\Gamma}_{pm} | P_{\text{eq}}^{\text{ext}} \delta d_{pm}^2 \rangle / \overline{[\delta d_{pm}^2(\beta_{n,\text{mol}})]^2}, \tag{4.15}$$

where $\hat{\Gamma}_{pm}$ is a reduced diffusion operator. Both a_{pm} and τ_{pm} can easily be calculated in terms of the chain order parameter S_0, which is the equilibrium value of $D_{00}^2(\Omega_{n,\text{mol}})$. If we define

$$b_{pm} = \tau_{pm}^{-1} + (D_\parallel - D_\perp)m^2 \tag{4.16}$$

the spectral density J_p^i can be written as

$$J_p^i(\omega) = \sum_{m=-2}^{2} a_{pm}\left[\frac{(S_m^i)^2 b_{pm}}{\omega^2 + b_{pm}^2} + j_m^i(\omega - ib_{pm})\right] + \delta_{p,0}(S_0)^2 j_0^i(\omega - ib_{p0}), \tag{4.17}$$

with $j_m^i(\omega)$ the Fourier-Laplace transform of the correlation function for the internal motion $g_m^i(t)$. In conclusion, it can easily be shown that the experimental data can be interpreted in terms of the three independent parameters S_0, $D_\parallel$, and $D_\perp$, all related to the overall motion of the system, in addition to the quantities for the internal motions already introduced.

In the previous derivation, it has been assumed that the preferred orientation of the molecule is the one with the all-*trans* axis normal to the bilayer surface. Actually, experimental results[44] just show that, in contrast with the gel, the liquid crystalline phase is characterized by axial symmetry on the time scale of NMR measurements. In principle, this does not necessarily imply that the all-*trans* axis tends to align with the bilayer normal, provided that a fast reorientation randomizes the polar angle of this axis in a frame having the Z axis along the bilayer normal. However, it should be pointed out that, as a first approximation, if the orienting field is assumed to obey some symmetry requirements, the results are almost independent of the particular model,[20] since in general, the decay of the correlation functions can be approximated by single exponentials, and the only independent parameters which enter into the calculation are S_0, $D_\parallel$, and $D_\perp$.

In general, for a Larmor frequency of 10–50 MHz, all the contributions appearing in Eq. (4.17) have to be taken into account. Accurate analysis of experimental data, based on fitting procedures, should be performed in order to obtain detailed dynamical information. However, some general features can be deduced from the expressions for the spectral densities and the theoretical values of conformational rates and internal order parameters. Experimental determinations[45–47] show that the spin–lattice relaxation times T_1 are longer than T_2 for all the positions in the chain by two orders of magnitude or more. This can only be explained as the effect of a slow motion (with a characteristic frequency low-

er than ω_D), which makes the zero frequency spectral densities $J_p^i(0)$, appearing only in the expression for T_2^i, larger than any other term. If the only relaxation mechanisms were the internal motions and the overall diffusion, the slow motion could be identified with the reorientation of the long molecular axis with respect to the bilayer normal, characterized by the diffusion coefficient $D_\perp$. If this is the case, the terms depending only upon the overall motion are expected to prevail over the others in the expression for the zero frequency spectral densities, because of the relatively large values of the typical frequencies for internal rotations. In particular, if the ratio $D_\parallel/D_\perp$ is sufficiently large, the decay constant τ_{p0}^{-1} becomes much smaller than τ_{p1}^{-1} and τ_{p2}^{-1}, so that the dependence of the relaxation rates T_2^{i-1} on position is expected to follow that of the internal order parameters S_{CD}^i.

Figures 9 and 10, respectively, show the T_1 and T_2 values that are calculated for a few choices of the motional parameters for the different positions of the chain. All the calculations have been performed for $\omega_D = 0.03w$, $S_0 = 0.7$, $(e^2qQ/h) = 10^6$ rad s^{-1}, and $\beta_{\text{lab},n} = 90°$. Actually, most of the available experimental data come from spectra of unoriented multilamellar dispersions, corresponding to a random distribution of director orientations; however, the prominent features in deuterium powder-type spectra are the sharp edges corresponding to $\beta_{\text{lab},n} = 90°$. In case (a), values of $D_\parallel = 0.1w$ and $D_\perp = 0.05w$ have been used. For such a low ratio of the diffusion coefficients, the calculated values of T_1^i and T_2^i are essentially the same. As mentioned above,

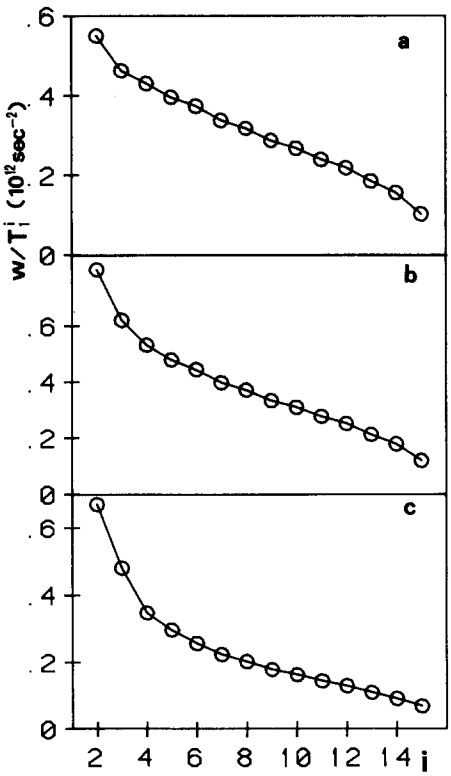

FIG. 9. Plot of $1/T_1$, calculated for $\beta_{\text{lab},n} = 90°$, $D_\parallel = 0.1w$ and different values of $D_\perp$. (a) $D_\perp = 0.05w$. (b) $D_\perp = 0.005w$. (c) $D_\perp = 0.0005w$. For comparison with experiment let w be of the order of 10^{10} s^{-1}.

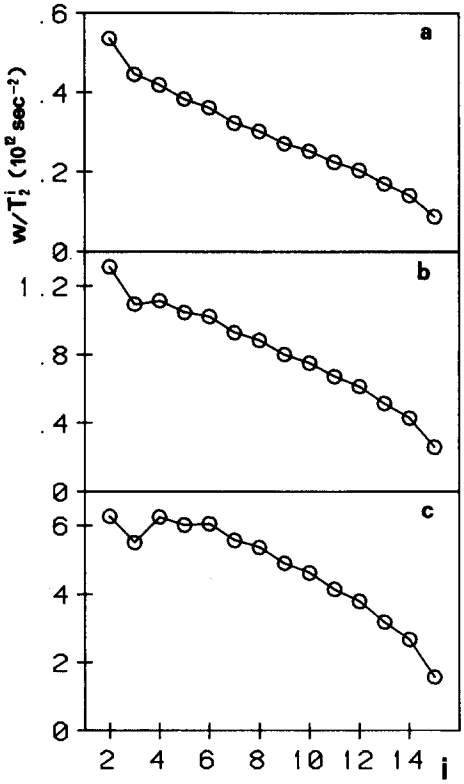

FIG. 10. Plot of $1/T_2$, calculated for $\beta_{\text{lab},n} = 90°$, $D_\parallel = 0.1w$ and different values of $D_\perp$. (a) $D_\perp = 0.05w$. (b) $D_\perp = 0.005w$. (c) $D_\perp = 0.0005w$. For comparison with experiment let w be of the order of 10^{10} s^{-1}.

the value of $D_\perp$ must be smaller than ω_D in order to significantly affect the ratio T_1^i/T_2^i. This becomes evident in case (b), where a value of $D_\perp = 0.005w$ has been assumed. Because of the decreased value of $D_\perp$, there is a larger contribution of the chain tumbling motion to the zero frequency spectral densities. As a consequence, the T_2^i values become smaller, even if their general trend is still similar to that of the T_1^i's. The spin–lattice relaxation times are less affected, except for the last positions of the chain, where the terms accounting for the overall motion have a relatively larger weight. In the extreme case (c) a value of $D_\perp = 0.0005w$ has been used. As expected, the very slow reorientation of the long molecular axis now has a dramatic effect on T_2^i; the ratio T_1^i/T_2^i varies from 10 to 30 along the chain, going from the fixed end towards the free one. The variations of the relaxation time T_2^i along the chain indeed show the same behavior seen for the internal order parameters S_{CD}^i. The spin–lattice relaxation times T_1^i are not so easy to analyze, because of the mixing of different contributions. It is possible, however, to deduce that the effect of the overall motion is larger as one moves in the direction of the free end of the chain. This is a consequence of the large increase of the internal kinetic parameters, which reduces the contribution of the internal motions to T_1^i, compared to the decrease in internal order parameters, which reduces the contribution of the overall motion to T_1^i.

Since, in principle, the full angular dependence of the relaxation times could be explored in oriented samples, calculations have been performed at different values of the an-

gle $\beta_{lab,n}$. The results obtained for the same parameters used in case (b) are reported in Fig. 11, the three series of data referring to $\beta_{lab,n} = 0°$, 30°, and 60°, respectively. It is interesting to note the large effect on the T_2^i's, whereas the T_1^i's are almost unaffected. Again, the explanation is found in the different weight of the contributions from overall and internal motions in the expression for the spectral densities. For $\omega \neq 0$ there is a predominance of the contributions resulting from the fast internal motions and described by the spectral densities j_m^i. These values do not change very much with the index m for a given segment; as a consequence the spectral densities J_p^i also have a very weak dependence upon the index p. On the other hand, at zero frequency there are larger contributions from the relatively slow overall motion, which modulates the residual segmental orderings not averaged to zero by the conformational kinetics, and these terms have markedly different effects on the different p components of the spectral densities J_p^i. It is important to point out that the above considerations hold in general for T_1, whereas the behavior of T_2 depends strongly on the choice of the parameters $D_\parallel$ and $D_\perp$, with no angular dependence being observed unless $D_\perp$ is of the order of ω_D. It is interesting to note that attempts to measure the angular dependence of the spin–lattice relaxation times on powder dispersion samples in the liquid crystal phase show that the T_1^i are indeed angle independent within an error of 10%.[48] This result has been explained as a consequence of a fast lateral diffusion, which would allow a rapid exchange of phospholipids among different orientations of the bilayer. On the basis of our calculation, the reason for the experimental observation would be the intrinsically weak angular dependence of the spin–lattice relaxation times.

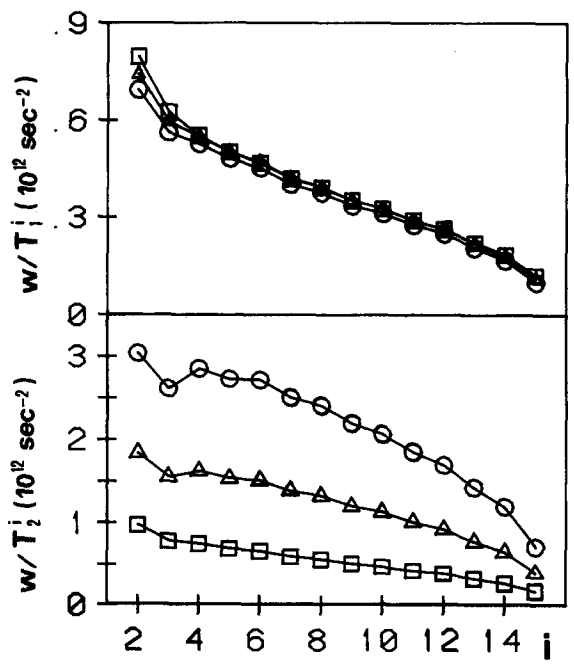

FIG. 11. Plots of $1/T_1$ and $1/T_2$ at various angles $\beta_{lab,n}$ (between the static magnetic field and the director) for the same conditions as case (b) of Figs. 9 and 10. Note that the circles are for $\beta_{lab,n} = 0°$, the triangles for $\beta_{lab,n} = 30°$, and the squares are for $\beta_{lab,n} = 60°$.

Finally, it should be pointed out that the frequency dependence of the relaxation times, which has attracted much attention in experimental studies,[3,35,49] eludes any simple analytical expression according to the present model, because of the many terms contributing and because of the complex frequency dependence of the spectral densities for the internal motions.

V. CONCLUSIONS AND COMMENTS

The salient features of the calculated macroscopic properties are essentially determined by only three parameters, all of which are well defined at a molecular level: $v_g = V_g / k_B T$, the energy of the *gauche* state relative to the *trans* state; $\epsilon^* = \epsilon / k_B T$, the strength of the orientational pseudopotential, and ρ, the ratio of the curvatures for the reactive and nonreactive modes. This latter parameter accounts for the degree of cooperativity of the torsional motions. Note that the elementary *gauche–trans* isomerization rate w, defined by Eq. (3.5), appears as a scaling parameter, containing both the energy barrier and the effective viscosity of the medium. Although the Pastor–Venable–Karplus potential used in the BD calculations is more detailed than the parametrized form adopted here, the static and dynamic properties calculated look very much the same. This implies that the basic ingredients are indeed contained in the ME method, and that special details not included in our model most likely do not alter the main picture that is obtained from the ME solutions. In particular, the close similarity of the position dependence of the order parameters [see Fig. 4 of Ref. 3(a)], indicates that the exclusion of configurations containing adjacent *gauche* states (as a result of the value of the van der Waals radius adopted here) has essentially the same effect as the repulsive part of the field proposed by Marcelja and included in the BD calculations. This view is also supported by the successful reproduction of the experimental chain length, discussed in Sec. IV A. However, the experimental data do not provide unambiguous choices for all parameters, and in fact, it has been shown for a $N = 10$ chain that the van der Waal radius r_0 can be substantially decreased, *provided* that the field parameter ϵ is moderately increased, without appreciably altering both static and dynamic properties.[26] Given these observations, the use of the simplest model appears to be a most reasonable choice.

There is one difference which concerns the order parameter, $\overline{D_{20}^2}$, which were found to decrease faster along the chain in the BD calculations than in the RIS model [Table I of Ref. 3(b)]. This is because these averages calculated according to the RIS approximation do not fully take into account the complete distribution of torsional angles. However, whereas this result shows a limitation of the RIS approximation, it is not necessarily true of the dynamical ME approach. In principle, one could more accurately compute the site values f_J of any function $f(\alpha)$, by using their full definition provided by the projection procedure of the diffusion equation onto the subspace of the localized functions [Eq. (10b) of Ref. 16(b)]. This is equivalent to considering the distribution of torsional angles about the location

α^J of the potential minima, instead of using the simple RIS approximation $f_J \cong f(\alpha^J)$. We have not done this in the present case because it is our belief that the rapid rotations about the long chain axis wash out the contributions of the order parameters $\overline{D^2_{20}}$ to the motional spectral densities.

The kinetic constants calculated by the BD and ME methods are indeed very similar. This was already noticed in a previous work, where the results of a simple Monte Carlo procedure[15] for the chain in isotropic environments were compared with Fig. 11 of Ref. 3(a). Therefore, one can safely conclude that multiple or concerted transitions cannot be of significance. Moreover, crankshaft and kink motions are definitely ineffective in causing NMR spin relaxation, both because of their low statistical weight and the fact that their time scale is slower than that of the $g \rightleftharpoons t$ transitions, at least in the plateau region where cooperativity makes the transition rates independent of the tail length. In agreement with the fruitful investigations started by Helfand and Skolnick,[10] the cooperativity of the single conformational events definitely rules out the relevance of multiple transitions in the chain dynamics.

Finally, the average internal correlation times reported in Fig. 6 of Ref. 3(b) are practically identical with those obtained by the ME procedure; (the nonmonotonic behavior along the chain in the BD calculations can be ascribed to poor statistics). For both techniques, the ratio of the average correlation times at the positions C_2 and C_{15} is 39. This is a proof that the bending modes and the possible couplings of jiggering motions in the potential wells do not appreciably contribute to the chain flexibility. The basic assumptions of the ME treatment, namely that the conformational kinetics is unaffected by the high-frequency motions, can therefore be safely accepted.

A general remark which emanates from the results of this work is that the same underlying physical processes may manifest themselves in different forms when different experimental techniques are used in the investigations. Thus, the theoretical calculations show that cooperativity in the torsional motions has the effect of leveling off the *gauche–trans* transition rates in the various positions of the chain. Although these motions are responsible for the decay of the correlation functions for the Wigner matrices related to specific tensorial interactions, the position dependence of the effective correlation rates does not exhibit a flat region, because the rotational motion of a particular bond is affected by the rotations of all segments connecting that bond to the fixed end. A second point worth mentioning is that the conformational dynamics is relatively insensitive to the presence of an anisotropic environment, despite the fact that static properties such as segmental order parameters are drastically changed in going from the isotropic to the LC phase.

If the theoretical results, obtained by considering both conformational motions and chain reorientations, are compared with the experimental observations derived from NMR measurements, the behavior of the deuterium longitudinal relaxation times is, in general, well understood. Relaxation effects measured on ^{13}C are expected to be essentially similar, but they have not been explicitly considered here, because the experimentally available data with natural isotopic abundance are unable to selectively distinguish the most interesting positions 4–13 of the chain. Except for the initial chain segments, the deuterium T_1 relaxation times increase continuously along the chain towards the free end, and exhibit only a weak angular dependence as the magnetic field is rotated with respect to the bilayer normal. The interpretation of T_2 is more intriguing. The experimental data on T_2 may be rationalized within the framework of our model by requiring a relatively low value of $D_\perp$, thereby predicting T_2's much shorter than T_1's. This is not the only mechanism that preferentially affects the near-zero (or zero) frequency spectral densities. As we have already mentioned, slow collective fluctuations, or slow rotations induced by lateral diffusion in unaligned samples, may contribute to the zero frequency values of the spectral densities, because of their frequency dispersion in the kilohertz regime.[49] In principle, the collective fluctuations might be distinguished from the slow chain tumblings by their different angular dependences.[50,51] In fact, Watnick *et al.*[47] interpret their short T_2's as due to collective fluctuations, but we note that their experiments appear to be characterized by orientation-*independent* T_2's. In that study $T_{1\rho}$ was also measured for a spin-locking frequency of $\omega'/2\pi = 50$ kHz. It was found to be more nearly equal to T_1 than to T_2. Therefore, one can conclude that the slow process should have its characteristic frequencies less than this value of ω'. We also note that there are fast motional processes, i.e., rapid fluctuations within the torsional potential wells, which could be affecting the NMR relaxation, and they might be detectable by techniques such as Raman or neutron scattering.

There are, of course, complementary studies by ESR (including orientation dependence), which have been interpreted in terms of decreased ordering and increased motional rates as one moves in the direction of the free end of the chain,[36,52] and this is consistent with our present model. ESR probes the dynamics on a faster time scale than NMR and can, therefore, supply complementary insights. It is believed that the ESR line shapes are particularly sensitive to the overall rotational dynamics,[36,52] and that the collective fluctuations are relatively unimportant. More detailed predictions of ESR relaxation in the context of the present model await the results of a synthesis of the slow-motional theory of line shapes[42] with the present theoretical model. In fact, because of the subtle mixing of spin degrees of freedom with the classical molecular dynamics in the slow-motional regime, one cannot simply use the classical correlation functions of the dynamics. This precludes the use of BD, whereas the ME approach conveniently allows for the required synthesis.[29,30,53]

A final interesting observation concerns the rapid convergence in the computation of the spectral densities for all the correlation functions with the LA. That is, a very small number of steps, at most of the order of 10–20, is required. The low dimensionality of the optimal reduced subspaces generated by the LA, compared with the huge dimensions of the whole problem, clearly indicates the existence of a few dominant modes. Their determination would be of much interest to better understand the physical processes, and to aid in overcoming the computational complexity. At pres-

ent, no complete analysis of this matter has been made. Nevertheless, it is possible to gain some insight from the behavior of the different correlation functions. First of all, we note that the functions representing unbalanced *gauche* populations are approximately eigenfunctions in absence of the mean field potential; in an oriented phase this is no longer true, but the corresponding spectral densities converge much faster than those of any other function, viz. only about 10 LA steps are sufficient to ensure an error less than 1%. Accordingly, the frequency dependence of the spectral densities for the functions $\mathscr{P}_g^i$ does not deviate appreciably from monoexponentiality, the larger deviations being observed for the central bonds. The spectral densities for the functions $\mathscr{P}_t^i$ exhibit a somewhat slower convergence, and a wider dispersion of relaxation rates. About 10–20 steps are required to yield convergence of the spectral densities for the angular functions, to the same error of 1%. Their frequency dependence shows that there are contributions of several motions with different time scales for all the segments but the first ones. These observations suggest that the relevant modes should be local in character, since functions describing local properties exhibit the fastest convergence. This suggests that the vectors $\mathscr{P}_t^i$ and $\mathscr{P}_g^i$ might be used individually as zero-order approximations for the evaluation of the kinetic constants, or globally as a truncated basis for the calculation of orientational correlation functions. Such a hypothesis agrees with the results obtained for a simple model of a chain of linear rotors,[15] where there is no conformational dependence of the friction matrix, and the problem can be factorized for the single rotors. As a consequence, all the dynamical properties are immediately interpreted in terms of local modes. Clearly, it would be of some interest to identify the key normal modes for the various correlation functions, a matter that we plan to explore with current computational methods.[29,30,53]

ACKNOWLEDGMENTS

A. F., G. J. M., and P. L. N. acknowledge the financial support of the Italian Ministry of Public Education and the National Research Council, through its Centro Studi sugli Stati Molecolari. R. H. C. and J. H. F. acknowledge the financial support of the National Institutes of Health (Grant No. GM-25862), and the National Science Foundation (Grants No. DMR-86-04200 and No. CHE 87-03014). Computations were performed at the Cornell National Supercomputer Facility funded by NSF and IBM Corp.

[1]J. H. R. Clarke and D. Brown, Mol. Phys. **58**, 815 (1986).
[2]P. van der Ploeg and H. J. Berendsen, J. Chem. Phys. **76**, 3271 (1982); **89**, 3718 (1988).
[3](a) R. W. Pastor, R. M. Venable, and M. Karplus, J. Chem. Phys. **89**, 1112 (1988); (b) R. W. Pastor, R. M. Venable, M. Karplus, and A. Szabo, *ibid.* **89**, 1128 (1988).
[4]P. J. Flory, *Statistical Mechanics of Chain Molecules* (Interscience, New York, 1969).
[5]D. J. Wallach, J. Chem. Phys. **47**, 5258 (1967).
[6]Y. K. Levine, N. J. M. Birdsall, A. G. Lee, and J. C. Metcalfe, J. Chem. Phys. **60**, 2890 (1974).
[7]R. E. London and J. Avitabile, J. Am. Chem. Soc. **99**, 7765 (1977); **100**, 7159 (1978).
[8]R. J. Wittebort and A. Szabo, J. Chem. Phys. **69**, 1722 (1978); R. J. Wittebort, A. Szabo, and F. R. N. Gurd, J. Am. Chem. Soc. **102**, 5723 (1980).
[9]O. Edholm and C. Blomberg, Chem. Phys. **42**, 449 (1979).
[10]J. Skolnick and E. Helfand, J. Chem. Phys. **72**, 5489 (1980); E. Helfand and J. Skolnick, J. Chem. Phys. **77**, 5714 (1982).
[11]J. S. Langer, Phys. Rev. Lett. **121**, 1668 (1961).
[12]R. Kimmich, G. Schnur, and A. Scheuermann, Chem. Phys. Lipids **32**, 271 (1983).
[13]H. Traüble, J. Membrane Biol. **4**, 193 (1971).
[14]A. Ferrarini, G. Moro, and P. L. Nordio, Mol. Phys. **63**, 225 (1988); in *Chemical Reactivity in Liquids: Fundamental Aspects,* edited by M. Moreau and P. Turq (Plenum, New York, 1988); G. Moro, A. Ferrarini, A. Polimeno, and P. L. Nordio, in *Reactive and flexible molecules in liquids,* edited by T. Dorfmüller (Kluwer Academic, Dordrecht, 1988).
[15]A. Ferrarini, G. Moro, P. L. Nordio, and A. Polimeno, Chem. Phys. Lett. **151**, 531 (1988).
[16](a) G. Moro and P. L. Nordio, Mol. Phys. **56**, 253 (1985); (b) **57**, 947 (1986); (c) Z. Phys. B **64**, 217 (1986).
[17]F. Coletta, G. Moro, and P. L. Nordio, Mol. Phys. **61**, 1259 (1987); F. Coletta, A. Ferrarini, and P. L. Nordio, Chem. Phys. **123**, 397 (1988).
[18]G. Moro, Chem. Phys. **118**, 167 (1987); **118**, 181 (1987).
[19](a) N. O. Petersen and S. I. Chan, Biochemistry **16**, 2657 (1977); (b) R. J. Pace and S. I. Chan, J. Chem. Phys. **76**, 4228 (1982).
[20]A. Szabo, J. Chem. Phys. **81**, 150 (1984).
[21]M. Karplus and J. N. Kushick, Macromolecules **14**, 325 (1981).
[22]R. A. Scott and H. A. Scheraga, J. Chem. Phys. **42**, 2209 (1965); **44**, 3054 (1966).
[23]D. Steele, J. Chem. Soc. Faraday Trans. **81**, 1077 (1985).
[24]S. Marcelja, Biochim. Biophys. Acta **367**, 165 (1974); Nature **241**, 451 (1973).
[25]J. W. Emsley, G. R. Luckhurst, and C. P. Stockley, Proc. R. Soc. London Ser. A **381**, 117 (1982).
[26]A. Ferrarini, Ph.D. thesis, University of Padova, 1989.
[27]M. E. Rose, *Elementary Theory of Angular Momentum* (Wiley, New York, 1957).
[28]EISPACK, Argonne Code Center, Argonne National Laboratory.
[29]G. Moro and J. H. Freed, J. Chem. Phys. **74**, 3757 (1980).
[30]G. Moro and J. H. Freed, in *Large Scale Eigenvalue Problems,* edited by J. Cullum and R. A. Willoughby (North-Holland, Amsterdam, 1986).
[31]J. Cullum and R. A. Willoughby, *Lanczos Algorithm for Large Symmetric Eigenvalue Computations* (Birkhauser, Basilea, 1985).
[32]D. C. Knauss and G. T. Evans, J. Chem. Phys. **73**, 3423 (1980).
[33]A. Seelig and J. Seelig, Biochemistry **13**, 4839 (1974).
[34]J. H. Davis, Biochem. Biophys. Acta **737**, 117 (1983).
[35]M. F. Brown, A. A. Ribeiro, and G. D. Williams, Proc. Natl. Acad. Sci. USA **80**, 4325 (1983); M. F. Brown, J. F. Ellena, C. Trindle, and G. D. Williams, J. Chem. Phys. **84**, 465 (1986).
[36]L. Kar, E. Ney-Igner, and J. H. Freed, Biophys. J. **48**, 560 (1985).
[37]M. A. Hemminga, Chem. Phys. Lipids **32**, 323 (1983).
[38]T. P. Higgs and A. L. McKay, Chem. Phys. Lipids **20**, 105 (1977).
[39]G. Zaccai, G. Buldt, A. Seelig, and J. Seelig, J. Mol. Biol. **134**, 693 (1979).
[40]A. Abragam, *The Principles of Nuclear Magnetism* (Oxford University, London, 1961).
[41]P. L. Nordio and U. Segre, in *The Molecular Physics of Liquid Crystals,* edited by G. R. Luckhurst and G. W. Gray (Academic, New York, 1979).
[42]J. H. Freed, G. V. Bruno, and C. F. Polnaszek, J. Phys. Chem. **75**, 3385 (1971).
[43]G. Moro and P. L. Nordio, Chem. Phys. Lett. **96**, 192 (1983).
[44]G. W. Stockton, C. F. Polnaszek, L. C. Leitch, A. P. Tulloch, and I. C. P. Smith, Biochem. Biophys. Res. Commun. **60**, 844 (1974).
[45]J. H. Davis, Biophys. J. **27**, 339 (1979).
[46]C. Mayer, K. Muller, K. Weisz, and G. Kothe, Liquid Crystals **3**, 797 (1988).
[47]P. I. Watnick, P. Dea, A. Nayeem, and S. I. Chan, J. Chem. Phys. **86**, 5789 (1987).
[48]M. F. Brown and J. Davis, Chem. Phys. Lett. **79**, 431 (1981).
[49]E. Rommel, F. Noack, P. Meier, and G. Kothe, J. Phys. Chem. **92**, 2981 (1988).
[50]P. L. Nordio and U. Segre, Gazz. Chim. Ital. **106**, 431 (1976).
[51]J. H. Freed, J. Chem. Phys. **66**, 4183 (1977).
[52]H. Tanaka and J. H. Freed, J. Phys. Chem. **88**, 6633 (1984).
[53]D. J. Schneider and J. H. Freed, Adv. Chem. Phys. **73**, 387 (1989).